

Fermi Surface and Band Renormalization in (Sr,K)Fe₂As₂ Superconductor from Angle-Resolved Photoemission Spectroscopy

Haiyun Liu¹, Wentao Zhang¹, Lin Zhao¹, Xiaowen Jia¹, Jianqiao Meng¹, Guodong Liu¹, Xiaoli Dong¹, G. F. Chen², J. L. Luo², N. L. Wang², Wei Lu¹, Guiling Wang³, Yong Zhou³, Yong Zhu⁴, Xiaoyang Wang⁴, Zuyan Xu³, Chuangtian Chen⁴, X. J. Zhou^{1,*1}

1

¹*National Laboratory for Superconductivity, Beijing National Laboratory for Condensed Matter Physics, Institute of Physics, Chinese Academy of Sciences, Beijing 100190, China*

²*Beijing National Laboratory for Condensed Matter Physics, Institute of Physics, Chinese Academy of Sciences, Beijing 100190, China*

³*Key Laboratory for Optics, Beijing National Laboratory for Condensed Matter Physics, Institute of Physics, Chinese Academy of Sciences, Beijing 100190, China*

⁴*Technical Institute of Physics and Chemistry, Chinese Academy of Sciences, Beijing 100190, China*

(Dated: July 20, 2008)

High resolution angle-resolved photoemission measurements have been carried out on (Sr,K)Fe₂As₂ superconductor ($T_c=21$ K). Three hole-like Fermi surface sheets are resolved for the first time around the Γ point which is consistent with band structure calculations. One electron-like Fermi surface and strong Fermi spots are observed near the $M(\pi,\pi)$ point. The overall electronic structure, particularly near the M point, shows significant deviations from the band structure calculations. The obvious bandwidth renormalization suggests the importance of electron correlation in understanding the electronic structure of the Fe-based compounds.

PACS numbers: 74.70.-b, 74.25.Jb, 79.60.-i, 71.20.-b

The recent discovery of superconductivity in iron-based ReFeAs(O,F) (Re represents rare earth elements like La,Ce,Pr,Nd,Sm and etc.) [1, 2, 3, 4, 5, 6] and (A,K)Fe₂As₂ (A represents alkaline earth elements like Ba and Sr)[7, 8, 9, 10] has attracted great attention because they represent second class of high temperature superconductors after the discovery of first high temperature superconductivity in cuprates[11]. Different from the cuprates where the parent compound is a Mott insulator[12], the parent compounds of the iron-based superconductors show a metallic behavior with a spin-density-wave ground state[13, 14, 15]. This has raised an important question on whether one should treat iron-based compounds with an itinerant electron model[16, 17] or localized correlated model[18, 19, 20, 21]. Direct measurement of the electronic structure is crucial in addressing this issue, and particularly the effect of electron correlation in this iron-based system[22, 23, 24].

In this paper, we report first direct measurements of the Fermi surface and band structure of the (Sr_{1-x}K_x)Fe₂As₂ superconductor by angle-resolved photoemission (ARPES) measurements. We have clearly identified three hole-like Fermi surface sheets near the Γ point of the Brillouin zone, which is consistent with the band structure calculations. We also observe an electron-like Fermi surface and strong Fermi spots near the $M(\pi,\pi)$ point. The overall electronic structure, particularly around the M point, shows significant difference from the band calculations. In addition, we observed an obvious bandwidth renormalization which suggests the importance of electron correlation in understanding the

electronic structure of the iron-based compounds. These results provide important information in establishing the basic electronic structure of the iron-based high temperature superconductors.

The angle-resolved photoemission measurements are carried out on our lab system equipped with Scienta R4000 electron energy analyzer with wide angle mode (30 degrees)[25]. We use Helium I resonance line as the light source which gives a photon energy of $h\nu=21.218$ eV. The light on the sample is partially polarized with the electric field vector mainly in the plane of the sample surface (as shown in Fig. 1a). The energy resolution was set at 12.5 meV and the angular resolution is ~ 0.3 degree. The Fermi level is referenced by measuring on the Fermi edge of a clean polycrystalline gold that is electrically connected to the sample. The (Sr_{1-x}K_x)Fe₂As₂ single crystals were grown using flux method [26] and the crystal measured has a superconducting transition at $T_c=21$ K[27]. The crystal was cleaved *in situ* and measured in vacuum with a base pressure better than 6×10^{-11} Torr.

Fig. 1 shows the Fermi surface (Fig. 1a), band structure (Figs. 1b and 1c) and corresponding photoemission spectra (energy distribution curves, EDCs)(Fig. 1d) on (Sr,K)Fe₂As₂ single crystal around the $\Gamma(0,0)$ point at a temperature of 45 K. The spectral weight distribution integrated over a narrow energy window $[-5\text{meV}, 5\text{meV}]$ near the Fermi level (Fig. 1a) gives a good representation of the measured Fermi surface. Three Fermi surface sheets can be clearly identified around the Γ point from Fig. 1a, as marked in Fig. 3. The first is the well-defined inner small Fermi surface sheet. The second is defined

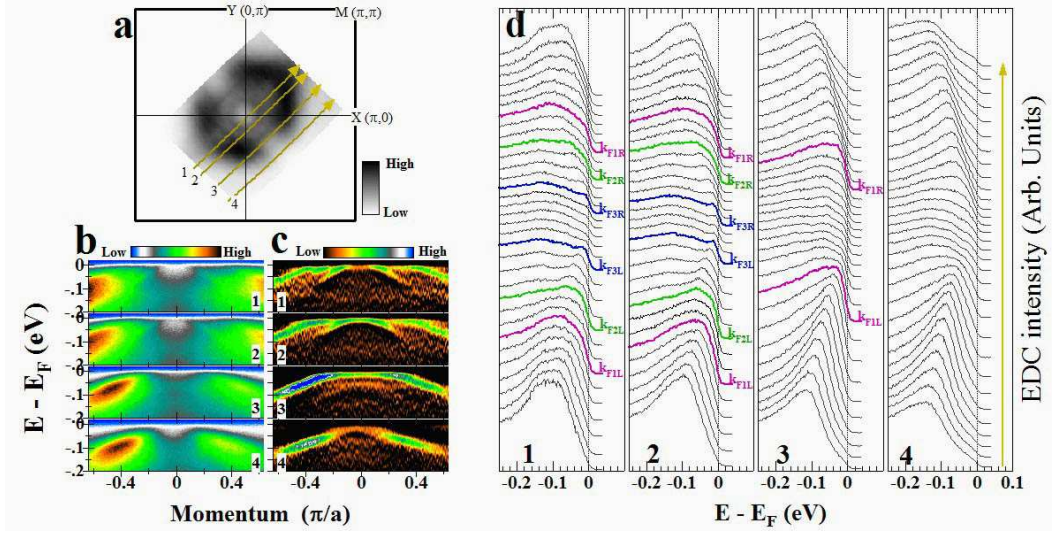


FIG. 1: Fermi surface, band structure and photoemission spectra of (Sr,K)Fe₂As₂ ($T_c=21$ K) near the Γ point measured at 45 K. (a). Spectral weight integrated within $[-5\text{meV}, 5\text{meV}]$ energy window with respect to the Fermi level as a function of k_x and k_y . The black arrow near the bottom-right marks the main electric field direction on the sample surface from the light source. (b). Original photoemission images measured along the four typical cuts as marked in Fig. 1a. (c). Corresponding second derivative images of Fig. 1b. (d). Photoemission spectra along the four cuts with EDCs at the Fermi momenta colored and marked.

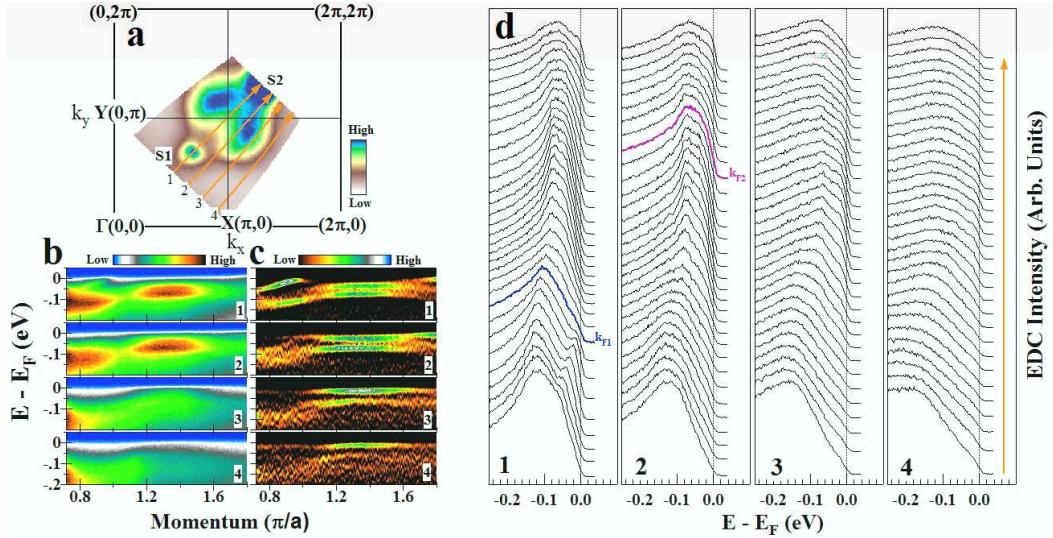


FIG. 2: Fermi surface, band structure and photoemission spectra of (Sr,K)Fe₂As₂ near the $M(\pi, \pi)$ point. (a). Spectral weight distribution integrated within $[-5\text{meV}, 5\text{meV}]$ energy window with respect to the Fermi level as a function of k_x and k_y . (b). Original photoemission images measured along the four typical cuts as marked in Fig. 2a. (c). Corresponding second derivative images of Fig. 2b. (d). Photoemission spectra along the four cuts with EDCs at the Fermi momenta colored and marked.

by nearly straight lines that can be clearly seen in Fig. 1a. The third Fermi surface sheet is defined by the outer strong intensity patches. We note that the overall spectral weight distribution is not symmetrical with four-fold symmetry with respect to the Γ point. This is due to photoemission matrix element effect because the main electric field component of the light is along one particu-

lar diagonal direction as marked in Fig. 1a.

Fig. 1b shows photoemission data taken along several typical momentum cuts as marked in Fig. 1a. The corresponding second derivative images, obtained by taking the second derivative on photoemission spectra with respect to the energy at each momentum, are shown in Fig. 1c. This is an empirical but effective way in highlighting

the underlying band structure[28]. From Fig. 1c, three Fermi crossings can be seen, as marked by three arrows on the data for the Cut 1, which correspond to three Fermi surface sheets near the Γ point. The measured bands further indicate that all the three Fermi surface sheets are hole-like. These band dispersions and the Fermi crossings can also be seen from the corresponding photoemission spectra for the four cuts with the EDCs at the Fermi crossings marked by colored lines (Fig. 1d). For the inner small Fermi sheet, clear EDC peaks are observed at the momentum crossings k_{F3L} and k_{F3R} in Fig. 1d for the Cuts 1 and 2.

Fig. 2 shows photoemission data of $(\text{Sr,K})\text{Fe}_2\text{As}_2$ measured around the $M(\pi,\pi)$ point at 45 K. The spectral weight distribution (Fig. 2a) shows two strong intensity spots, S1 and S2, along the $\Gamma(0,0)$ - $M(\pi,\pi)$ - $(2\pi,2\pi)$ line, with their locations nearly symmetrical with respect to the $M(\pi,\pi)$ point. On both sides of the $\Gamma(0,0)$ - $M(\pi,\pi)$ - $(2\pi,2\pi)$ line, there are two patches of strong intensity. The maximum intensity contours on the two patches are not enclosed and also the two strong intensity spots appear to be isolated from the patches. These give rise to some disconnected Fermi crossings identifiable around the $M(\pi,\pi)$ point, as marked in Fig. 3. From the band structure measurements (Fig. 2b and 2c), it is clear that the strong intensity spot, S1 in Fig. 2a, originates from the band near the upper-left corner of Figs. 2b and 2c for the Cut1. From Fig. 2c, it is also clear that, near the $M(\pi,\pi)$ point, the main electronic features are the two flat bands which are ~ 30 meV and ~ 80 meV below the Fermi level. The ~ 30 meV band crosses the Fermi level and forms an electron-like Fermi surface sheet near the $M(\pi,\pi)$ point that correspond to the contour of the maximum intensity contour of the two patches (as marked in Fig. 3a near M point).

Fig. 3 summarizes the overall Fermi surface of $(\text{Sr,K})\text{Fe}_2\text{As}_2$ by combining both measurements around the Γ (Fig. 1a) and M point (Fig. 2a). Three hole-like Fermi surface sheets are resolved around the Γ point for the first time, different from two Fermi surface sheets observed in $(\text{Ba,K})\text{Fe}_2\text{As}_2$ compounds[23, 24]. Interestingly, the shape of the three Fermi surface sheets appear to be not circular, but more like squares. The enclosed area of the inner, middle and outer Fermi sheets are ~ 0.06 , ~ 0.28 , ~ 0.52 , respectively, with a unit of $(\pi/a)^2$. On the other hand, for the M point, there is an electron-like Fermi surface sheet associated with the Fermi crossings on the strong intensity patches (as marked near the M point in Fig. 3a). However, because the patches are not enclosed near the M point probably due to the matrix element effect, and the appearance of two strong Fermi spots, S1 and S2, we need to further determine whether the two strong spots and the patches are independent or they belong to the same electron-like Fermi surface sheet. Fig. 3(b-d) shows spectral weight distribution integrated over different energy ranges away from the Fermi level.

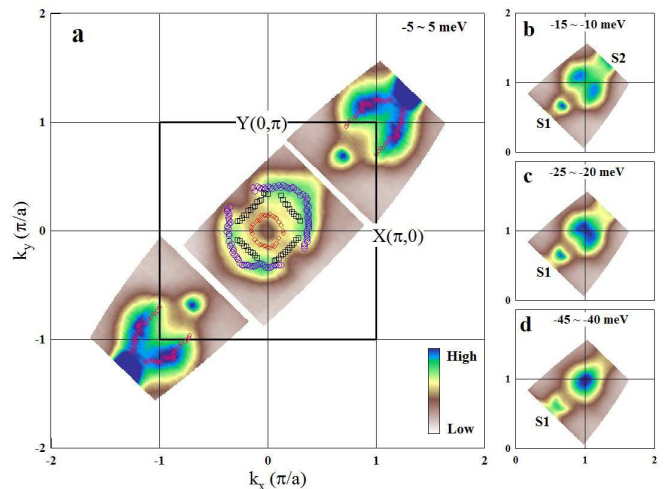


FIG. 3: Fermi surface of $(\text{Sr,K})\text{Fe}_2\text{As}_2$. (a). Spectral weight distribution integrated over a small energy window $[-5\text{meV}, 5\text{meV}]$ with respect to the Fermi level. The Fermi momenta are marked by symbols. (b), (c) and (d) show spectral weight distribution near the $M(\pi,\pi)$ point integrated over energy windows of $[-15\text{meV}, -10\text{meV}]$, $[-25\text{meV}, -20\text{meV}]$ and $[-45\text{meV}, -40\text{meV}]$, respectively, with respect to the Fermi level.

The strong Fermi spot S1 moves away from the M point with increasing binding energy, which is consistent with the band dispersion as seen from Fig. 2b and 2c (Cut 1, up-left band). On the other hand, the electron-like Fermi surface defined by the patches gradually shrinks towards the M point. This clearly indicates that the two strong Fermi spots S1 and S2 are independent from the electron-like Fermi surface sheet defined by the patches near the M point.

Fig. 4 shows an overall band structure of $(\text{Sr,K})\text{Fe}_2\text{As}_2$ along typical high symmetry lines. This measurement, together with Fermi surface information (Figs. 1, 2 and 3) makes it possible to have a direct comparison with theoretical calculations. Since there is no band calculations available on $(\text{Sr,K})\text{Fe}_2\text{As}_2$ and it is expected that the band structure of SrFe_2As_2 is similar to that of BaFe_2As_2 [30], we take the band calculations of BaFe_2As_2 [24, 30, 31] for comparison. The observation of three hole-like Fermi surface sheets near the Γ point is consistent with the band calculations[30]. However, the overall measured band structure and Fermi surface show significant difference from the band calculated results[24, 30, 31], particularly around the M point. As shown in Fig. 4c, four bands are expected from band calculations near the M point within 0.6 eV energy range, with two bands near -0.2 eV that give rise to two electron-like Fermi surface sheets around the M point[30]. This is quite different from the experimental results where only two shallow flat bands are observed near ~ -0.03 eV and ~ -0.08 eV and only one Fermi surface sheet is identified.

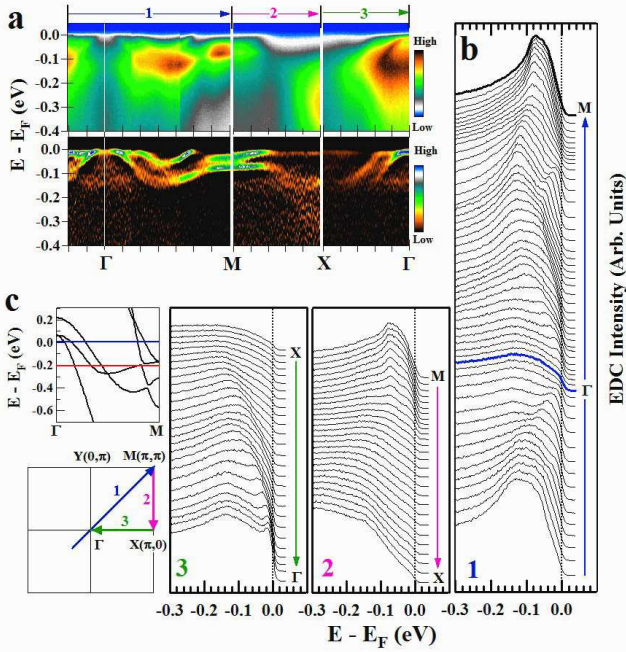


FIG. 4: Energy bands of (Sr,K)Fe₂As₂ along high-symmetry lines. (a). Original photoemission images (upper panels) and the corresponding second derivative images (lower panels) [29]. The locations of the momentum cuts are marked in the left-bottom inset. (b). Corresponding photoemission spectra. The corresponding momentum range is marked on top of Fig. 4a. (c). Calculated band structure along the Γ -M direction in BaFe₂As₂ [30].

Moreover, the extra band along the Γ -M cut (Fig. 4a) that gives rise to the strong Fermi spots in the Fermi surface mapping (Fig. 1a) is not present in the band calculation (Fig. 4c).

The deviation between the measured and calculated electronic structure may arise from a couple of reasons. First, there may be appreciable uncertainty in the band calculation itself. For instance, for the same BaFe₂As₂, the calculation by Liu et al. [24] gives only two Fermi crossings around the Γ point while three crossings are expected from calculations of other groups [30, 31]. Second, there can be some uncertainty caused by k_z dispersion. For a given photon energy as we used, the measured electronic structure corresponds to one particular k_z with its location to be determined. However, we believe this may not be the main reason because the bands near the M point are not strongly sensitive to k_z [30, 31]. Third, the effect of chemical potential shift has to be taken into account. The potassium (K⁺) doping in the (Sr,K)Fe₂As₂ sample introduces holes and is expected to lower the chemical potential compared with the parent compound. By carefully examining the measured band structure (Fig. 4a) and the calculated one (Fig. 4c) [30], we find that a qualitative agreement between the mea-

sured and calculated electronic structure seems to be possible if one assumes a chemical potential shift down by ~ 0.2 eV (as marked by a red line in Fig. 4c): (1). There are still three hole-like Fermi surface sheets around the Γ point; (2). There is one extra band along Γ -M which resembles the one in Fig. 4a that gives rise to strong Fermi spots in Fermi surface mapping (Fig. 2a); (3). Near the M point, this would lead to two bands with one band crossing the Fermi level to give an electron-like Fermi surface.

We note that while qualitative consistency may be realized by shifting the chemical potential, there remain quantitative discrepancies between the measured and calculated electronic structures, such as the exact location of the Fermi crossings which determines the area of the Fermi surface, that needs further theoretical investigations. One particularly notable difference between the measurement and the calculations is the width of the band dispersion. As seen from Fig. 4c, the major occupied bands along Γ -M cut are spread within 0.6 eV energy range for BaFe₂As₂, while they are within 0.15 eV in the measured data (Fig. 4a). Even considering possible 0.2 eV chemical potential shift, there remains obvious narrowing in the measured band width compared with the calculated one. This appreciable band renormalization suggests that electron correlation needs to be taken into account in describing the electron structure of the Fe-based compounds.

In summary, our angle-resolved photoemission measurements have provided detailed electronic structure of the (Sr,K)Fe₂As₂ superconductor. Significant deviation between the measured and calculated electronic structure is revealed that asks for further theoretical efforts. The obvious bandwidth renormalization suggests the importance of electron correlation in understanding the electronic structure of the Fe-based compounds.

We thank Xiaogang Wen, Dunghai Lee, Zhong Fang, and Junren Shi for helpful discussions. This work is supported by the NSFC, the MOST of China (973 project No: 2006CB601002, 2006CB921302), and CAS (Projects ITSNE).

*Corresponding author: XJZhou@aphy.iphy.ac.cn

-
- [1] Y. Kamihara et al., J. Am. Chem. Soc. **130**, 3296 (2008).
 - [2] X. H. Chen et al., Nature **453**, 761 (2008).
 - [3] G. F. Chen et al., Phys. Rev. Lett. **100**, 247002 (2008).
 - [4] Z. A. Ren et al., Europhys. Lett. **82**, 57002 (2008).
 - [5] Z. A. Ren et al., arXiv:cod-mat/0803.4283.
 - [6] Z. A. Ren et al., Chin. Phys. Lett. **25**, 2215 (2008).
 - [7] M. Rotter et al., arXiv:cod-mat/0805.4630.
 - [8] K. Sasmal et al., arXiv:cod-mat/0806.1301.
 - [9] G. F. Chen et al., arXiv:cod-mat/0806.1209.
 - [10] G. Wu et al., arXiv:cod-mat/0806.1459.
 - [11] J. G. Bednorz et al., Z. Phys. B **64**, 189 (1986).

- [12] P. A. Lee et al., Rev. Mod. Phys. **78**, 17 (2006).
- [13] J. Dong et al., Europhys. Lett. **83**, 27006 (2008).
- [14] C. Cruz et al., Nature **453**, 899(2008).
- [15] M. Rotter et al., arXiv:cod-mat/0805.4021.
- [16] D. J. Singh and M.-H. Du, Phys. Rev. Lett. **100**, 237003 (2008).
- [17] H. J. Zhang et al., arXiv:cod-mat/0803.4487.
- [18] K. Haule et al., Phys. Rev. Lett. **100**, 226402(2008).
- [19] C. Cao et al., Phys. Rev. B **77**, 220506R (2008).
- [20] Z. P. Yin et al., arXiv:cond-mat/0804.3355.
- [21] F. J. Ma et al., arXiv:cond-mat/0804.3370.
- [22] C. Liu et al., arXiv:cond-mat/0806.2147.
- [23] L. X. Yang et al., arXiv:cond-mat/0806.2627.
- [24] C. Liu et al., arXiv:cond-mat/0806.3453.
- [25] G. D Liu et al., Rev. Sci. Instruments **79**, 023105 (2008).
- [26] G. F. Chen et al., arXiv:cod-mat/0806.2648.
- [27] The precise K content in the $(\text{Sr}_{1-x}\text{K}_x)\text{Fe}_2\text{As}_2$ ($T_c=21$ K) is to be determined. From the $T_c \sim x$ curve[8] it is estimated to be $x \sim 0.25$. It is underdoped compared with optimal doping at $x=0.4$ with a $T_c=38$ K.
- [28] W. T. Zhang et al., Phys. Rev. Lett. **101**, 017002 (2008).
- [29] The X-M measurement is obtained from Y-M measurement which can be slightly different due to matrix element effect from particular light polarization and sample measurement geometry.
- [30] I. A. Nekrasov et al., arXiv:cod-mat/0806.2630.
- [31] F. J. Ma et al., cond-mat/0806.3526.